Modeling, Analysis and Design of Centrifugal Force Driven Transient Filling Flow into Rectangular Microchannel

Dong Sung Kim and Tai Hun Kwon

Dept. of Mechanical Engineering, Pohang University of Science and Technology (POSTECH),
San 31 Hyoja-dong Nam-gu, Pohang, Kyungpuk, 790-784, Korea, thkwon@postech.ac.kr

ABSTRACT

In this paper, we *first* present successful modeling and analysis results of a *centrifugal force driven transient filling flow* into a *rectangular* microchannel. Two types of exact and pseudo-static approximate solutions were derived for the transient filling flow. The analytic solutions include expressions for flow front advancement, detailed velocity profile and pressure distribution. The obtained analytical results show that the filling flow driven by centrifugal force is affected by three dimensionless parameters which combine fluid properties, rectangular channel geometry and processing condition of rotational speed. We also *first* provide a simple *analytical design tool for a rectangular microchannel* based on the modeling and analysis in this study.

Keywords: Transient flow, Centrifugal force, Rectangular microchannel, Analysis, Design

1 INTRODUCTION

Recently, centrifugal pumping is regarded as an excellent alternative control method of the fluid flow inside microchannels [1-3]. The centrifugal force generates fluid flow with little sensitivity to the physicochemical properties of the working fluid, such as ionic strength, pH and so on [1]. It can also provide parallel pumping flows to several microchannels simultaneously on the same CD type microfluidic chip. It is important to understand the spatial and temporal behavior of fluid flow inside the microchannel for a precise design of a centrifugal microfluidic channel system. So far, most of previous studies in the literature simply adopted capillary stop valves making use of a surface tension effect for the purpose of controlling fluid flow, with lack of detailed understanding of the centrifugal flow behavior. In this regard, we have provided the analysis results and design tool for a transient filling flow into a *circular* microchannel via centrifugal force [4]. However, the cross-sectional geometry of microchannels which were fabricated by the conventional photolithography is usually rectangular in most practical cases. It might be possible to apply the analytical results for the circular microchannel to the design of arbitrary cross-sectional microchannels, such as a trapezoidal cross-sectional microchannel, based on the definition of the hydraulic radius. But, the analytical solutions for the rectangular microchannel are definitely useful and precise to understand and design the flow inside the rectangular microchannel [5]. In this regard, we report the analysis results and design tool for a centrifugal force driven transient filling flow into a *rectangular* microchannel in this study.

2 PROBLEM STATEMENT

Figure 1 shows a schematic diagram of a rectangular cross-sectional microchannel on a CD type microfluidic chip. Suppose a sample fluid of density, ρ, and viscosity, μ, is injected into a reservoir located at L_0 from the center of the CD. Now consider the fluid flow when a rotational motor starts rotating the CD plate in a constant rotational speed of ω. The material will flow out of the reservoir into the microchannel due to the centrifugal force and the flow front gradually advances along the radial direction of the CD plate. It is of our interest to be able to determine the flow front advancement as a function of the time t, denoted by $l(t)$. Of course, this flow front advancement will depend on the rotational speed, ω, as well as the location of reservoir, rectangular microchannel geometry and fluid material properties.

As for the design aspect, in order to deliver a sample to a *desired position,* L_d at a *desired time,* t_d, a designer has to decide where to put the reservoirs (L_0), the widths and heights of the microchannels (W and H) for each channels along with the rotational speed (ω) of the disk.

3 MODELING AND ANALYSIS

The dimensionless governing equations for this centrifugal force driven transient filling flow and the corresponding boundary conditions can be stated as (the superscript asterisk means dimensionless parameter):

$$ReG_A \frac{\partial w^*}{\partial t^*} - C_A{}^2 \frac{\partial^2 w^*}{\partial x^{*2}} - \frac{\partial^2 w^*}{\partial y^{*2}} = \frac{1}{2} ReG_A \overline{V}^2 \omega^{*2} \left(l^*(t^*) + L_0{}^* \right) \tag{1}$$

$$w^*(0, y^*, t^*) = 0,\ w^*(1, y^*, t^*) = 0 \tag{2a}$$

$$w^*(x^*, 0, t^*) = 0,\ w^*(x^*, 1, t^*) = 0 \tag{2b}$$

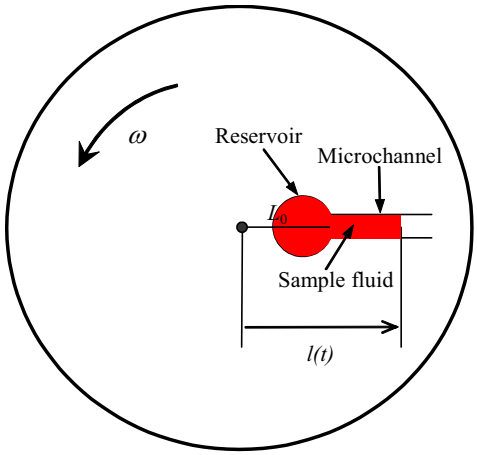

Figure 1: Schematic diagram of the transient filling flow into a rectangular microchannel on the rotating CD type microfluidic chip. Dark red area represents a region occupied by the sample fluid. $l(t)$ indicates the flow front.

$$\frac{dl^*}{dt^*} = \int_0^1 \int_0^1 w^*(x^*, y^*, t^*)\, dx^* dy^* \tag{3}$$

$$l^*(0) = L_0^*, \tag{4}$$

$$p^*(z^*, t^*) = \overline{V}^2 \omega^{*2} \left(z^* - L_0^*\right)\left(z^* - l^*(t^*)\right) \tag{5}$$

where w, Re, G_A (=H/L), C_A (=H/W), $\overline{V}$ and p denote downchannel (the same as the radial direction of the CD) velocity, the Reynolds number, a geometrical aspect ratio, a channel aspect ratio, a ratio of rotational velocity to convective velocity and pressure, respectively.

In this study, two types of solutions for pseudo-static approximate (when the inertia term is neglected, i.e., $ReG_A << 1$) and exact cases were successfully derived based on the governing equations of Equations (1), (3) and (5) and the corresponding boundary conditions of Equations (2) and (4). The obtained pseudo-static ($w_{static}^*(x^*, y^*, t^*)$) and exact ($w^*(x^*, y^*, t^*)$) velocity profiles are:

$$w_{static}^*(x^*, y^*, t^*) = 16 ReG_A \overline{V}^2 \omega^{*2} L_0^* e^{D_{static} t^*} \cdot \sum_{m=1,3,5,\cdots}^{\infty} \sum_{n=1,3,5,\cdots}^{\infty} \frac{\sin m\pi x^* \sin n\pi y^*}{\lambda_{mn,static} mn\pi^2} \tag{6}$$

and

$$w^*(x^*, y^*, t^*) = 16 ReG_A \overline{V}^2 \omega^{*2} L_0^* e^{Dt^*} \cdot \sum_{m=1,3,5,\cdots}^{\infty} \sum_{n=1,3,5,\cdots}^{\infty} \frac{\sin m\pi x^* \sin n\pi y^*}{\lambda_{mn} mn\pi^2}, \tag{7}$$

where the exponents D_{static} and D are the most important parameters in this study of which the physical meaning is an *inverse of a characteristic time for flow advancement*, determined by

$$D_{static} = 32 ReG_A \overline{V}^2 \omega^{*2} \sum_{m=1,3,5,\cdots}^{\infty} \sum_{n=1,3,5,\cdots}^{\infty} \frac{1}{\lambda_{mn,static} m^2 n^2 \pi^4}$$

with $\lambda_{mn,static} = C_A{}^2 m^2\pi^2 + n^2\pi^2$ (8)

and

$$D = 32 ReG_A \overline{V}^2 \omega^{*2} \sum_{m=1,3,5,\cdots}^{\infty} \sum_{n=1,3,5,\cdots}^{\infty} \frac{1}{\lambda_{mn} m^2 n^2 \pi^4}$$

with $\lambda_{mn} = ReG_A D + C_A{}^2 m^2\pi^2 + n^2\pi^2$. (9)

Both pseudo-static and exact *filling flow advancements*, $l_{static}^*(t^*)$ and $l^*(t^*)$, respectively, were found to increase exponentially with the time as expressed by

$$l_{static}^*(t^*) = L_0^* \left[2e^{D_{static} t^*} - 1\right] \tag{10}$$

and

$$l^*(t^*) = L_0^* \left[2e^{Dt^*} - 1\right]. \tag{11}$$

The pressure distributions for both pseudo-static ($p_{static}^*(z^*, t^*)$) and exact ($p^*(z^*, t^*)$) cases were also derived as follows:

$$p_{static}^*(z^*, t^*) = \overline{V}^2 \omega^{*2} \left(z^* - L_0^*\right) \cdot \left[z^* + L_0^* - 2L_0^* e^{D_{static} t^*}\right] \tag{12}$$

and

$$p^*(z^*, t^*) = \overline{V}^2 \omega^{*2} \left(z^* - L_0^*\right)\left[z^* + L_0^* - 2L_0^* e^{Dt^*}\right]. \tag{13}$$

4 ANALYSIS RESULTS

Figure 2 shows the effects of ReG_A and $\overline{V}\omega^*$ on D with regard to both D_{static} and D when C_A was kept to 0.2 (Equations (8) and (9)). The effect of ReG_A on $l^*(t^*)$ for the both pseudo-static and exact filling flow advancements is shown in Figure 3 when $\overline{V}\omega^* = 1$ and C_A=0.2 (Equations (10) and (11)). Figure 4(a) shows a typical 3-dimensional exact velocity profile when ReG_A=10, $\overline{V}\omega^* = 0.2$ and C_A=0.2 at t^*=80 and also Figures 4(b) and 4(c) show the effect of ReG_A on $w^*(x^*, y^*, t^*)$ with regard to the both pseudo-static and exact velocity profiles when $\overline{V}\omega^* = 1$ and C_A=0.2 at t^*=5 (Equations (6) and (7)). And finally, the change of the both pseudo-static and exact pressure distributions with respect to the variation of ReG_A is calculated based on Equations (12) and (13) when $\overline{V}\omega^*$=1 and C_A=0.2 at t^*=5, as shown in Figure 5.

Since the exponent D is proportional to the square of $\overline{V}\omega^*$ while it is linearly proportional to ReG_A, the flow characteristics are more sensitively affected by the change of $\overline{V}\omega^*$ than ReG_A as shown in Figure 2.

The calculated exact solutions coincide with the pseudo-static solutions as shown in Figures 2, 3, 4(b), 4(c) and 5 while $ReG_A \ll 1$ even at high $\overline{V}\omega^*$ since the exact solutions of D, $l^*(t^*)$, $w^*(x^*,y^*,t^*)$ and $p^*(z^*,t^*)$ asymptotically behave like the pseudo-static solutions of D_{static}, $l_{static}^*(t^*)$, $w_{static}^*(x^*,y^*,t^*)$ and $p_{static}^*(z^*,t^*)$ under the condition of $ReG_A \ll 1$. However, it should be noted that the higher ReG_A is, the more deviation between the pseudo-static and exact cases is, as clearly shown in Figures 2-5, due to the inertia force effect. The inertia force restrains a rapid velocity increase, thereby causing a smaller value of D (Figure 2) and slower advancement in the real exact flow than the pseudo-static approximate one (Figures 3 and 4). Therefore, the exact solution behaviors deviate more from the pseudo-static ones as ReG_A increases.

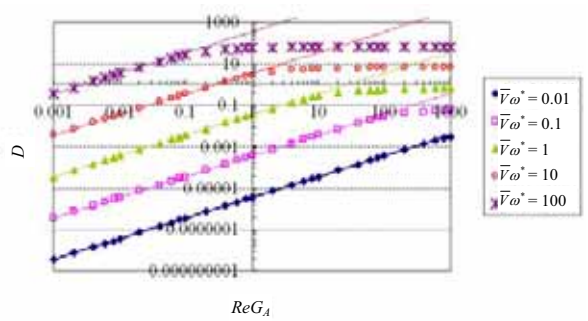

Figure 2: The calculated exponent D as a function of ReG_A for various $\overline{V}\omega^*$ when C_A=0.2 (*symbols* from transient D and *curves* from pseudo-static D_{static}).

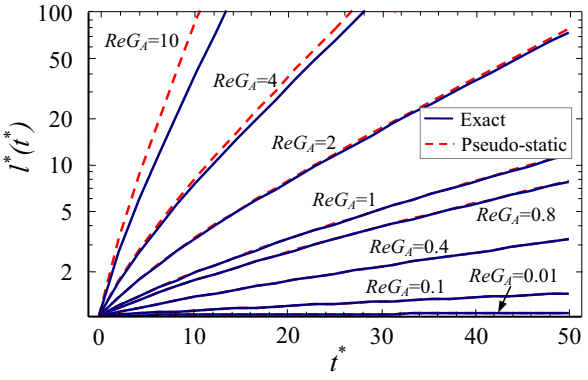

Figure 3: Effect of ReG_A on $l^*(t^*)$ when $\overline{V}\omega^* = 1$ and C_A=0.2 (*solid curves*: exact flow, *dotted curves*: pseudo-static flow).

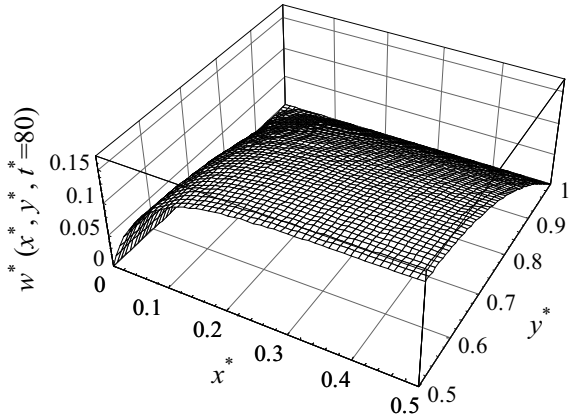

(a)

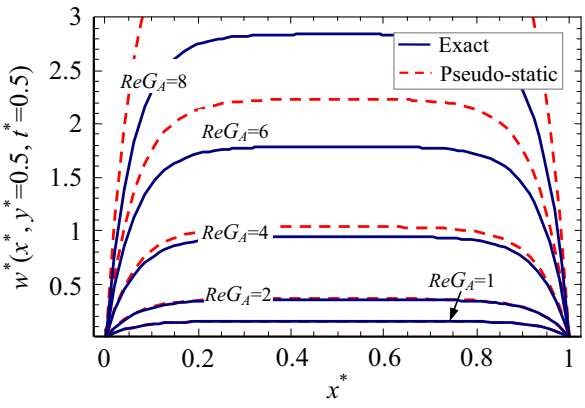

(b)

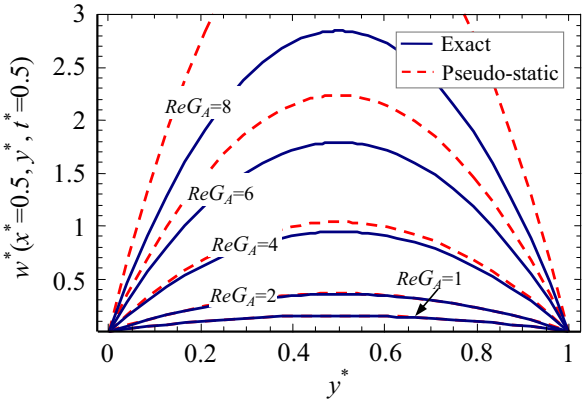

(c)

Figure 4: Velocity profiles, $w^*(x^*,y^*,t^*)$: (a) a typical 3-dimensional transient velocity profile when ReG_A=10, $\overline{V}\omega^* = 0.2$ and C_A=0.2 at t^*=80, (b) Effects of ReG_A when $\overline{V}\omega^* = 1$ and C_A=0.2 on velocity at y^*=0.5 and t^*=5, and (c) at x^*=0.5 and t^*=5 (*solid curves*: exact velocity, *dotted curves*: pseudo-static velocity).

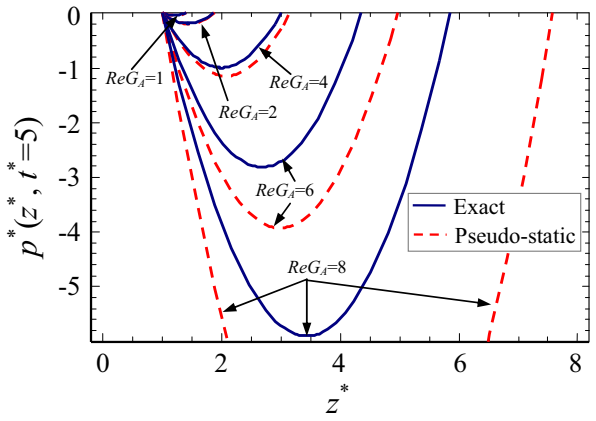

Figure 5: The change of pressure distribution for both cases of pseudo-static (dotted curves) and exact (solid curves) solutions with respect to the variation of ReG_A when $\overline{V}\omega^*$ =1 and C_A=0.2 at t^*=5.

5 DESIGN

Suppose a microfluidic designer wants to deliver a sample fluid from the reservoir location, L_0, to the desired radial downchannel location, L_d, at a desired time, t_d. Based on the analysis in this study, we have derived the following design equations to meet the design requirements:

Design Equation I:

$$D = \frac{1}{t_d} \ln\left[\frac{1}{2}\left(\frac{L_d}{L_0} + 1\right)\right] \tag{14}$$

Design Equation II:

$$D = \frac{32\rho\omega^2}{\mu} \sum_{m=1,3,5,\cdots}^{\infty} \sum_{n=1,3,5,\cdots}^{\infty} \frac{1}{\frac{D\rho}{\mu} + \left[\left(\frac{m\pi}{W}\right)^2 + \left(\frac{n\pi}{H}\right)^2\right] m^2 n^2 \pi^4} \tag{15}$$

For the given design requirements of L_0, L_d and t_d, a dimensional value of D can be easily determined by means of Equation (14) and then the width, W (or height, H), or the rotational speed, ω, is subsequently determined for given fluidic conditions, i.e., fluid density, ρ, and vicosity, μ, with the calculated D from the nonlinear equation of Equation (15).

Therefore, by means of the above *Design Equation I* and *Design Equation II* (Equations (14) and (15)), one can easily *determine W (*or *H)* or ω for the given fluid properties (ρ and μ), position of reservoir (L_0) and design requirements (L_d and t_d).

6 CONCLUDING REMARKS

In this paper, we have first developed the physical modeling and carried out the analysis for the centrifugal force driven transient filling flow into a rectangular microchannel. Two analytical solutions of exact and pseudo-static approximate cases were derived for this transient filling flow. The obtained analytical results show that the filling flow driven by centrifugal force is affected by three dimensionless parameters of ReG_A, $\overline{V}\omega^*$ and C_A which combine fluid properties, channel geometry and processing condition of rotating speed. We also first provide a simple analytical microchannel design equations to meet the design requirements based on the modeling and analysis in this study.

ACKNOWLEDGEMENT

The authors would like to thank the Korean Ministry of Science and Technology for the financial supports via the National Research Laboratory Program (2000-N-NL-01-C-148) and the Korean Ministry of Education & Human Resources Development supporting BK21 program.

REFERENCES

[1] D.C. Duffy, H.L. Gillis, J. Lin, N.F. Sheppard, Jr. and G.J. Kellogg, Anal. Chem., 71, 4669, 1999.
[2] M.J. Madou, L.J. Lee, S. Daunert, S. Lai and C.-H. Shih, Biomed. Microdevices, 3, 245, 2001.
[3] GyrolabTM Microlaboratory – www.gyros.com.
[4] D.S. Kim and T.H. Kwon, Proc. Micro Total Analysis Systems (μTAS) 2004, 1, 174, 2004; D.S. Kim and T.H. Kwon, Microfluid. Nanofluid., submitted.
[5] D.S. Kim, K.-C. Lee, T.H. Kwon and S.S. Lee, J. Micromech. Microeng., 12, 236, 2002.